AD_____

Award Number: DAMD17-01-1-0435

TITLE: Optimization of Breast Cancer Treatment by Dynamic Intensity Modulated Electron Radiotherapy

PRINCIPAL INVESTIGATOR: Dennis D. Leavitt, Ph.D.

CONTRACTING ORGANIZATION: University of Utah
Salt Lake City, Utah 84102-1870

REPORT DATE: October 2004

TYPE OF REPORT: Annual

PREPARED FOR: U.S. Army Medical Research and Materiel Command
Fort Detrick, Maryland 21702-5012

DISTRIBUTION STATEMENT: Approved for Public Release;
Distribution Unlimited

The views, opinions and/or findings contained in this report are those of the author(s) and should not be construed as an official Department of the Army position, policy or decision unless so designated by other documentation.

REPORT DOCUMENTATION PAGE

Form Approved
OMB No. 074-0188

1. AGENCY USE ONLY (Leave blank)	2. REPORT DATE	3. REPORT TYPE AND DATES COVERED
	October 2004	Annual (1 Oct 2003 - 30 Sep 2004

4. TITLE AND SUBTITLE
Optimization of Breast Cancer Treatment by Dynamic Intensity Modulated Electron Radiotherapy

5. FUNDING NUMBERS
DAMD17-01-1-0435

6. AUTHOR(S)
Dennis D. Leavitt, Ph.D.

7. PERFORMING ORGANIZATION NAME(S) AND ADDRESS(ES)
University of Utah
Salt Lake City, Utah 84102-1870

E-Mail: Dennis.leavitt@hci.utah.edu

8. PERFORMING ORGANIZATION REPORT NUMBER

9. SPONSORING / MONITORING AGENCY NAME(S) AND ADDRESS(ES)
U.S. Army Medical Research and Materiel Command
Fort Detrick, Maryland 21702-5012

10. SPONSORING / MONITORING AGENCY REPORT NUMBER

11. SUPPLEMENTARY NOTES

12a. DISTRIBUTION / AVAILABILITY STATEMENT
Approved for Public Release; Distribution Unlimited

12b. DISTRIBUTION CODE

13. ABSTRACT (Maximum 200 Words)

Since electron arc dose calculations using Monte Carlo are quite time-consuming, we have investigated "gross optimization" techniques that will allow determination of a set of starting parameters that can converge to final values within a few iterations. This will allow us to determine the final optimized leaf settings for each arc segment within a reasonable time. Included in this "gross optimization" will be use of precalculated fluence maps reflective of the treatment head geometry, so that the initial parameter set can be determined using Monte Carlo calculations only within the individual patient anatomy. These techniques will make determination of the final leaf settings very straightforward. Additionally, beam data sets have been verified for the clinical range of field sizes and energies. Lastly, we are working with Varian Medical Systems to determine a transition path from our one-of-a-kind electron arc configuration into a supportable system that can be readily available to the general radiotherapy community.

14. SUBJECT TERMS	15. NUMBER OF PAGES
Electron arc therapy, optimization	18
	16. PRICE CODE

17. SECURITY CLASSIFICATION OF REPORT	18. SECURITY CLASSIFICATION OF THIS PAGE	19. SECURITY CLASSIFICATION OF ABSTRACT	20. LIMITATION OF ABSTRACT
Unclassified	Unclassified	Unclassified	Unlimited

Table of Contents

INTRODUCTION

Subject: Electron Arc Therapy was developed to treat extended superficial volumes within the postmastectomy chest wall. Although this technique has been applied to other superficial disease sites, it has remained of primary application, at least in our department, to the postmastectomy chest wall. Unique advantages of this technique include 1) reduced dose inhomogeneity at abutment sites; 2) improved dose homogeneity across the extended chest wall; 3) limitation of dose to critical structures such as heart and lung; and 4) reduced dose to the apex of the lung through use of electrons rather than a photon field across this region. Limitations of this technique include 1) the extensive labor required to fabricate the secondary and tertiary field defining apertures; 2) extensive treatment planning time to calculate the electron arc dose distributions and to "optimize" the shape of the secondary aperture to deliver the desired uniform dose.

Purpose: The purpose of this work is to overcome the above listed limitations and to improve the treatment planning capability and dose delivery capability through implementation of **I**ntensity **M**odulated **E**lectron **R**adio**t**herapy **(IMERT).** Using methods similar to static field photon IMRT, IMERT will define the electron arc fields using the photon Multi-Leaf Collimator, will define the specific field shapes required as the gantry rotates around the patient, and will deliver specific dose components as required for each segment of arc. The specific field shapes defined by the MLC leaves, and the specific dose components required for each arc segment will be determined by the optimization code.

Scope: This work represents a unique extension of treatment planning and dose delivery tools for electron radiotherapy. This will be the first application of photon collimators to electron treatment, and will test the capability of Monte Carlo dose calculation codes to compute electron arc dose distributions in a reasonable length of time. We hope that the innovations developed in this work will eliminate the labor-intensive fabrication of secondary and tertiary field shaping devices, and will allow all field-shaping to be accomplished using the photon MLC and a simple accessory trimmer. The end product of this work will be a direct comparison of IMERT vs. standard post-mastectomy treatment techniques.

BODY: Five specific tasks were identified as part of this work:

1. Implement a 3-dimensional electron dose calculation model for the electron arc studies.
2. Measure the dose characteristics of electron beams defined by the photon MLC.
3. Confirm efficacy of 3-D dose calculations using phantoms simulating actual patient shapes.
4. Compare Dose-Volume-Histograms for target volume, heart, and lungs for IMERT vs. other chest wall radiation therapy techniques.
5. Test Clinical Applicability: Treatment Planning Time and Actual Treatment Time for **IMERT** vs. standard forward planning.

- **Dose Calculation Model:** In previous work we had investigated two-dimensional tabular models and 2 or 3-dimensional pencil beam models. The limitations of these models, particularly regarding definition of the fluence through the MLC, led us to investigate Monte Carlo methods for electron arc dose calculations. This model has been

implemented, based on the CNRC Monte Carlo code supported by Dr. Dave Rogers. We made no effort to "enhance" the code performance, but rather concentrated on implementing existing code. To improve the calculation time, we purchased over 25 PC's and linked them into an array to calculate the Monte Carlo dose distributions. Some features of the code that were not germaine to our calculation needs were disconnected in order to improve the performance. Some refinements that improve the performance of the code through the MLC have been made by Dr. Rogers' group. These have been implemented. Additionally, some enhancements to the code calculating dose within the patient have been developed by Dr. Rogers' group. These have yet to be implemented by us.

- **Electron Beam Dose Characteristics:** Ideally, we hope to use electron fields up to 40 cm long. In reality, the geometry of the Varian Clinac 2100CD produces "flat" electron fields only up to about 30 cm long. Beyond this length, the electron dose profile tails off to as little as 40% of maximum. This simply reflects the fact that the manufacturer did not require electron field flatness for fields larger than 30 cm x 30 cm. This is demonstrated in the long-axis dose profiles for 6 MeV, 9 MeV and 12 MeV that are attached as Figures 1, 2, and 3. In a review of patients treated using electron arc therapy, we have not found this to be a serious constraint, in that the cephalocaudad field length was always less than 30 cm. (Although not directly related to our work, we will contact users of other commercial brand clinical linear accelerators and ask whether their linacs produce longer regions of flat profile intensity.) We have encountered some problems in reproducing the extremes of the long-axis profiles, even using the Monte Carlo code. We believe this reflects the need to refine the specification of the ancillary components within the treatment head. Although all other components remain the same, the electron scattering foil assembly changes from energy to energy. The thickness and composition of primary and secondary scattering foil differs with energy, with a pyramid assembly common for the downstream foil. We still see some difference between calculated and measured profiles at the extremes of the cephalocaudal axis, but have chosen to not invest more time in these differences, since the extremes are outside the clinical limits defined by review of previously treated cases.
- **Efficacy of Dose Calculations:** To first order, the virtual source position for electrons is "downstream" approximately 12 cm from the source position for photons. This is the location of the electron scattering foils that sit on the same carousel as does the photon flattening filter. This means that there should be a discrepancy between the projected light field for electrons vs. the actual radiation field. This was verified by comparing a measured film density profile vs. calculated electron field for an unusual MLC configuration: All MLC leaves were closed; then leaves corresponding to off-axis distance of 0.5 cm, +/-9.5 cm, and +/-19.5 cm were opened to a width of 5 cm. A radiographic film was exposed using this MLC configuration, and the film was processed. The film image is shown in figure 4. This revealed that the electron field through each MLC leaf aperture projects a field approximately 5 cm wide in the cephalocaudal direction at the treatment plane, and that the deviation between the projected light field and the actual electron field increases with increasing leaf distance from central axis. This is in agreement with calculations, and validates the electron calculations.

This difference between light field projection and actual computed dose is significant for the dose optimization efforts. Since the width adjustment of any MLC leaf pair will impact the dose through planes up to +/- 3 cm from that leaf pair, the optimization schedule must simultaneously look at the effect of ANY leaf pair modification upon the entire volume. This means that simple plane-by-plane optimization will not succeed.

- **Optimization Techniques:** The optimization efforts for electron arc therapy differ from those using photons. In the electron arc therapy mode, specific reference points are entered at which the dose will be determined. These reference points are entered plane-by-plane, with inter-plane distances of either 0.5 cm or 1.0 cm. Within each plane, the reference points are distributed across the irradiated segment of the patient, at a depth corresponding to the dmax depth (depth of maximum dose) for the electron energy used in that segment. The electron arc is divided into as many as 16 segments (a limitation of our treatment planning system), and the dose to each reference point from each arc segment is calculated. This produces a large two-dimensional dose matrix of reference point doses. In simplest form, the width of each MLC leaf pair (separation of the opposed leaves) for each arc segment is adjusted until the dose at all reference points approaches, as closely as possible, the prescribed dose.

  We have investigated two general types of optimization techniques, a "global" calculation and a "gradient search" technique. Both techniques have, to date, been very time consuming. This time has been minimized by the observation noted above that the dose contribution from a single leaf pair extends through planes +/-3cm from that leaf pair. So the "global" search for any leaf pair can be limited to roughly six planes. A second promising approach pre-selects the starting leaf pair positions based on our observations from previous work. We noted that the change in dose is roughly linear as the leaf pair opening is increased. This observation allows us to precalculate the electron arc dose distribution for four rectangular field sizes, and then set the individual leaf-pair starting positions based on interpolation between these calculated doses. This is illustrated in the following example: For a patient treated using only 6 MeV arcs, the entire arc was divided into thirteen arc segments with all leaf pairs opened to project a 5 cm wide light field at isocenter. In the central plane, the relative weight attached to each arc segment was adjusted to deliver a uniform dose to the reference points in this plane. This calculation was then repeated using leaf pairs opened to 3 cm wide, 4 cm wide, then 6 cm wide. This range usually brackets the aperture widths applied to electron arc therapy. Figure 5 illustrates the relative dose profile along the reference points in the central plane for the four field widths. Figure 6 illustrates the relative dose profile for a plane 3 cm superior to the central axis plane. Similarly, figure 7 illustrates the dose profiles in a plane 8 cm superior to the central axis. Lastly, figure 8 shows the dose profile in a plane 6 cm inferior to the central plane. In this plane it is clear that the "gross optimization" technique has failed to choose the widths based on the correct plane. This demonstrates that some additional "tuning" is needed with this technique in order to make it more robust. At this point, these starting values are fed manually into the optimization search. This is a step that should be automated.

  We have found that a "dose-surface-map" can contribute as an important visual parameter of optimization. This allows the operator to drive the search in a direction

desired by interpreting the dose-surface-map. Figure (9) demonstrates the dose-surface-map for an "idealized" dose distribution, i.e., all reference points have the same dose. Figure (10) illustrates the dose-surface-map for an unoptimized calculation, i.e. dose due to arcing rectangular fields, unadjusted for change in radius of curvature. This illustrates that the initial variation in dose before any attempt at optimization by aperture adjustment is dramatic, ranging from +28% to – 27% about the desired dose. The average dose is 101%. By applying the interpolation technique described above the dose-surface-map is made more uniform, as illustrated in figure (11). In this case the maximum dose is reduced to +22% above the desired dose, while the minimum dose stubbornly remains at -25% below desired dose. The average dose is 99.5%. This clearly demonstrates that the interpolative gross optimization technique can provide a better starting point for the more time-consuming gradient search or global search techniques, but cannot by itself resolve the few outlying points at which dose remains exceptionally high or low compared to the desired dose.

The use of thirteen arc segments enabled a finer resolution in the leaf-pair openings vs. arc angle. However, we found that the projection of the individual leaf-pair openings would move from plane to plane as the shape of the patient contour changed across the arc. This made the initial estimation of the gross-optimization of leaf pairs more difficult. This is a problem that we will resolve by measuring the change in leaf-pair projection vs. depth of isocenter. When this table is completed, the initial estimate of leaf-pair openings will be much more reliable. This projection of the leaf-pair openings will also be energy dependent, since the scattering angle of the electrons decreases with increasing electron energy.

The results of this study indicate that we can estimate a starting leaf-pair configuration that will be used in the optimization routine, thereby eliminating several iterations corresponding to the initial search.

KEY RESEARCH ACCOMPLISHMENTS

- Devised "Gross Optimization" technique for fast determination of initial parameters for gradient search or global search optimization techniques.
- Confirmed efficacy of dose calculation models for electron arc therapy.
- Accumulated approximately half of required patient data sets for dose-volume-histogram studies.

REPORTABLE OUTCOMES

- Oral scientific presentation at AAMD (June 2005) and AAPM (July 2005).

CONCLUSIONS

We have demonstrated a "Gross Optimization" technique that, with some minor refinements, will dramatically minimize the search time required by either of the two optimization techniques we are employing for this study. This enhanced throughput will help to make this procedure a

clinically viable technique for treating breast cancer. We are confident that this keeps us on track toward a successful completion of the project within the extended period of the grant.

"SO WHAT SECTION":

Although the development of this electron arc therapy is a fascinating endeavor, we feel that it would be a horrible waste if it were to remain only an "intellectual curiosity" to the rest of the clinical radiotherapy world. We are therefore aggressively working with Varian Medical Systems to implement the linear accelerator modifications that will allow this to become a standard clinical tool. We feel, with all sincerity, that the success of this project will be judged by our ability to make it readily available to the rest of the radiotherapy community.

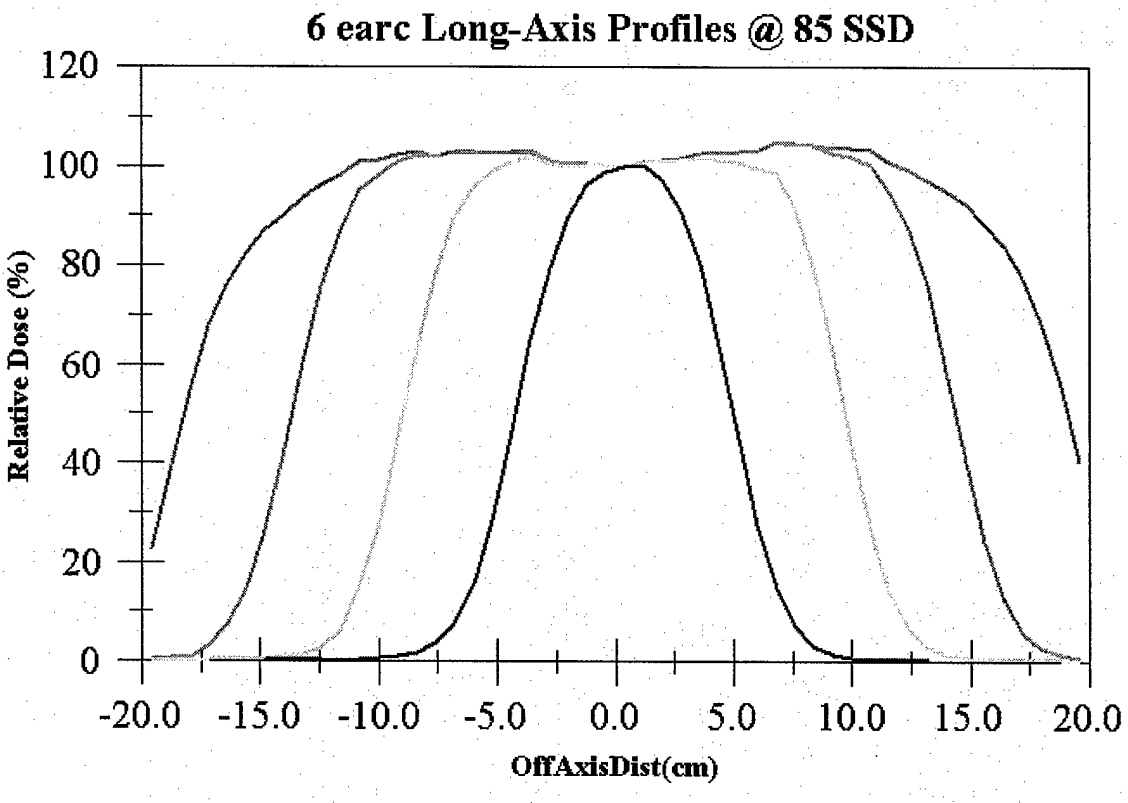

Figure 1: 6 MeV Long-Axis Profiles measured at 85 cm SSD for the MLC-defined aperture set to 39 cm, 30 cm, 20 cm, and 10 cm long by 5 cm wide. The "shoulder" is prominent in the 39 cm long profile, but does not contribute to the 30 cm long profile. In clinical applications to date, the 30 cm long profile is most commonly applied. These long-axis profiles are all defined using the divergent edge of the MLC leaf, rather than the rounded end of the leaf. The penumbra is therefore somewhat different.

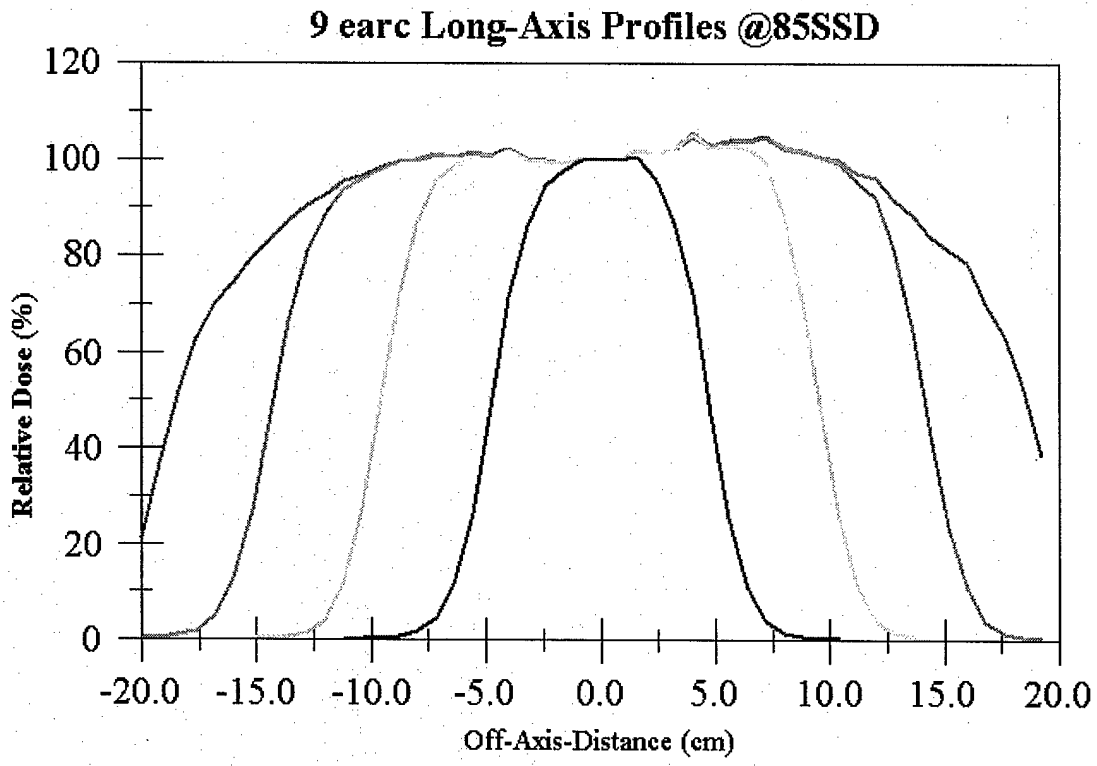

Figure 2: 9 MeV Long-Axis Profiles measured at 85 cm SSD for the MLC-defined aperture set to 39 cm, 30 cm, 20 cm, and 10 cm long by 5 cm wide. The "shoulder" is prominent in the 39 cm long profile, and introduces some rounding to the 30 cm long profile. The effect of electron energy on the electron scattering can be seen by the sharper penumbra of the 9 MeV long-axis profiles compared to the 6 MeV profiles.

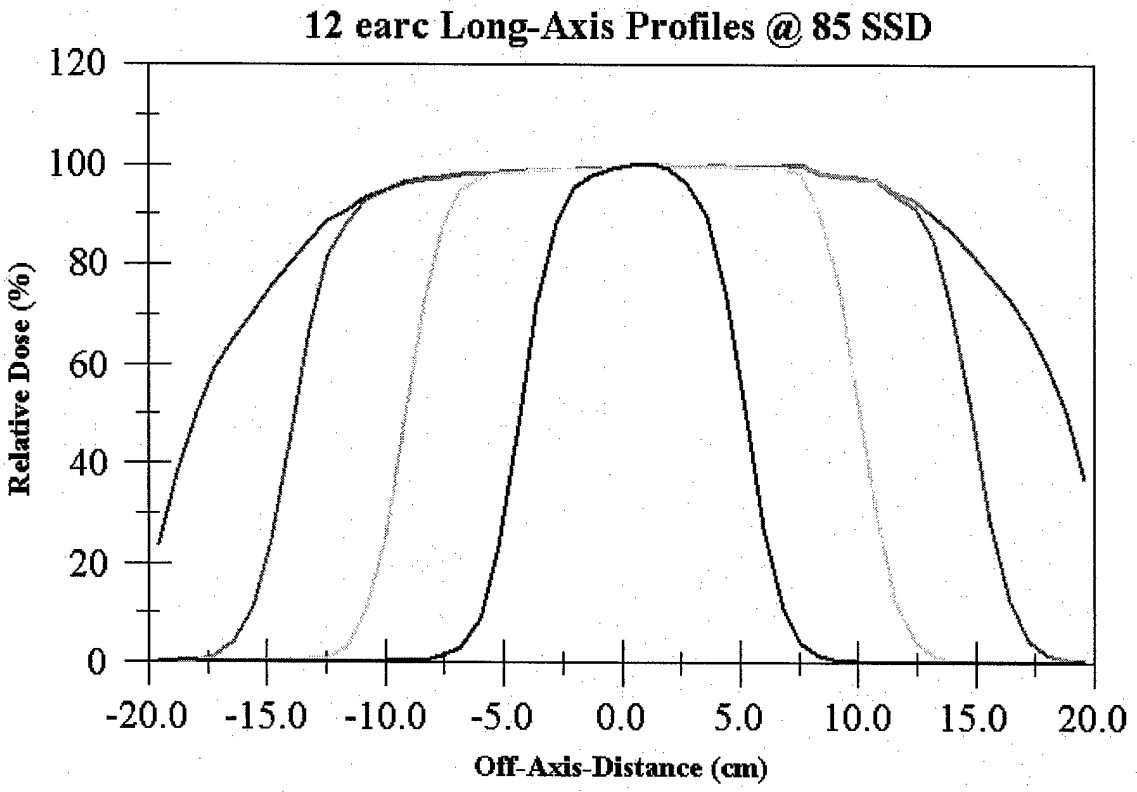

Figure 3: 12 MeV Long-Axis Profiles measured at 85 cm SSD for the MLC-defined aperture set to 39 cm, 30 cm, 20 cm, and 10 cm long by 5 cm wide. The "shoulder" is prominent in the 39 cm long profile, and introduces increased rounding to the 30 cm long profile. The effect of electron energy on the electron scattering can be seen by the sharper penumbra of the 12 MeV long-axis profiles compared to the 6 MeVand 9 MeV profiles.

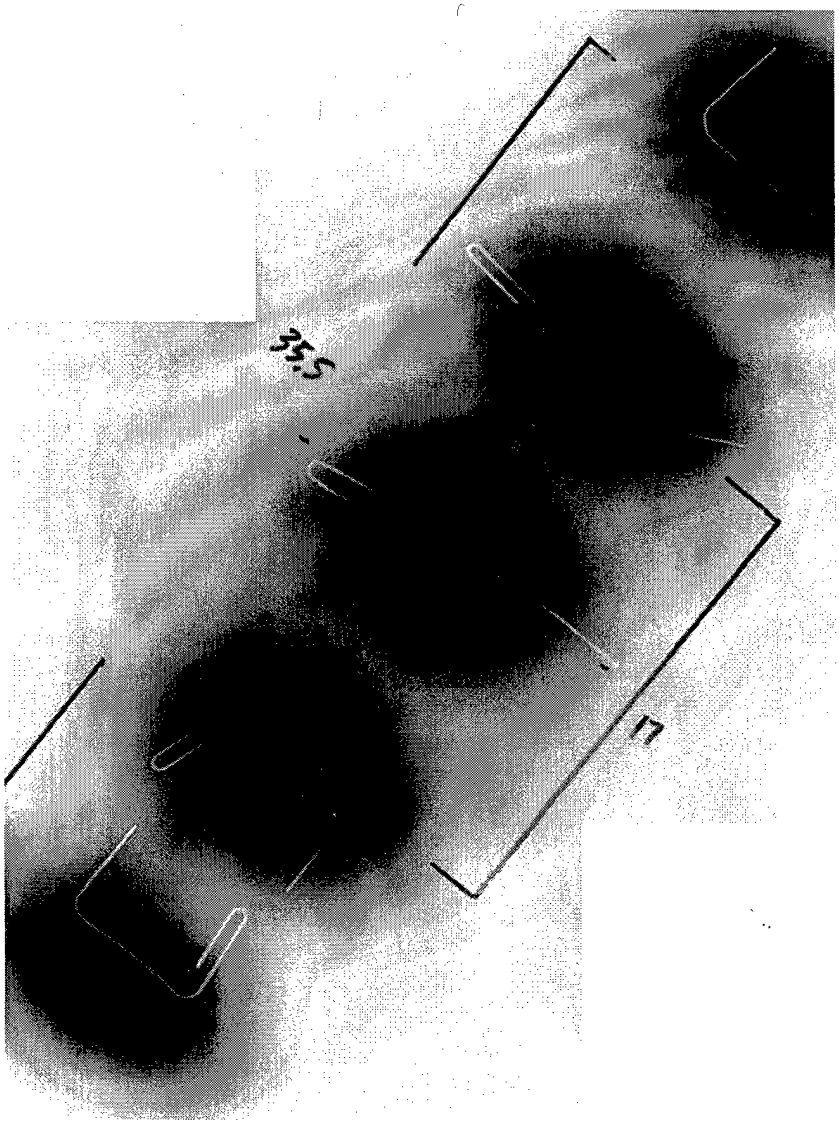

Figure 4: Film densitometric verification of divergence of electron dose field from projected light field. The light field is projected from the "target" position, 100 cm upstream from the isocenter. The electron field is projected effectively from the position of the electron scattering foil, which is 12 cm "downstream" from the target position. Since the photon jaw positions are set based on the light field, the electron field projection is greater as determined by simple geometry. Additionally, the electron field projected through each MLC leaf pair extends in the cephalocaudad plane through about 5 cm, thereby contributing to at least two planes above and below the central plane of interest. This limits the efficacy of the proposed "gross optimization" technique.

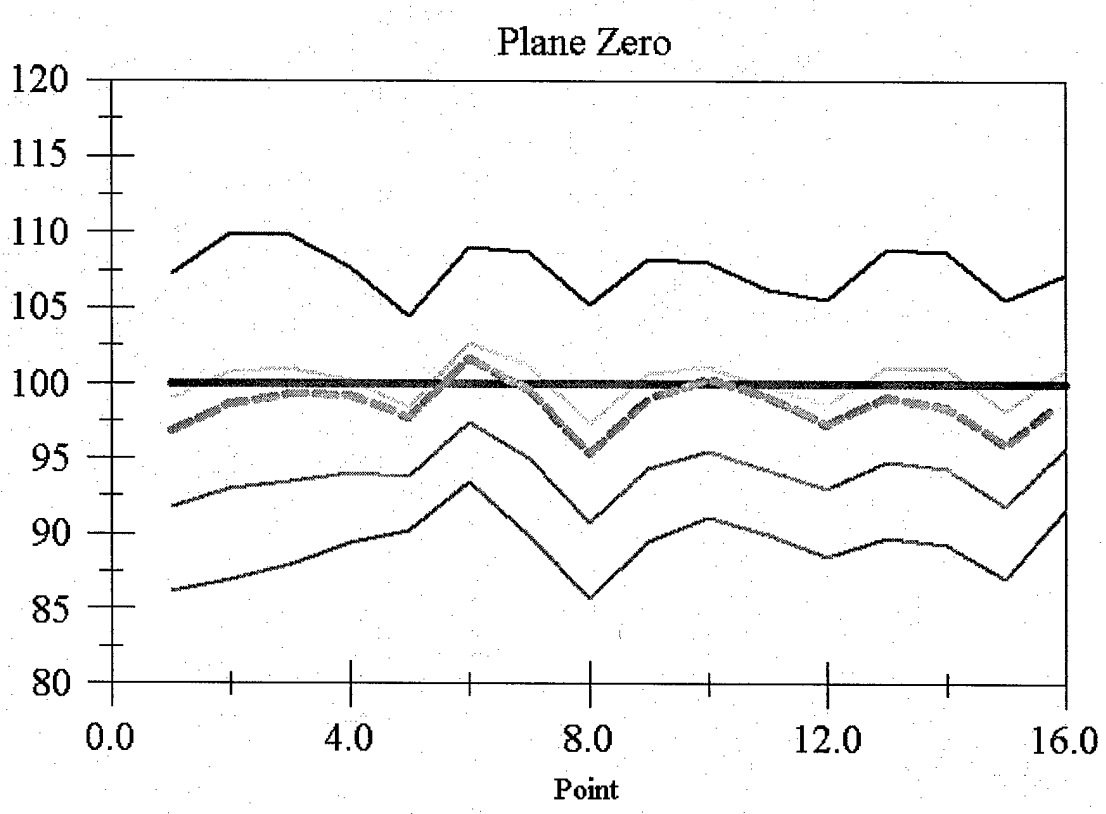

Figure 5: Dose profile in central axis plane for arcs defined using 3 cm, 4 cm, 5 cm, and 6 cm wide rectangular fields. The individual weight for each of the 13 arc segments has been adjusted to deliver the most uniform dose in the central axis plane using the 5 cm wide rectangular field. The solid horizontal line corresponds to the "ideal" dose distribution in this plane (100% at all reference points). The dashed line corresponds to the "gross optimization" dose distribution in this plane. Notice that, although the MLC leaves projecting through the central axis plane all project a 5 cm wide field, the dose in this plane has been modified by the different shapes projected in the planes immediately above and below this plane. This is common to all planes in the gross optimization technique.

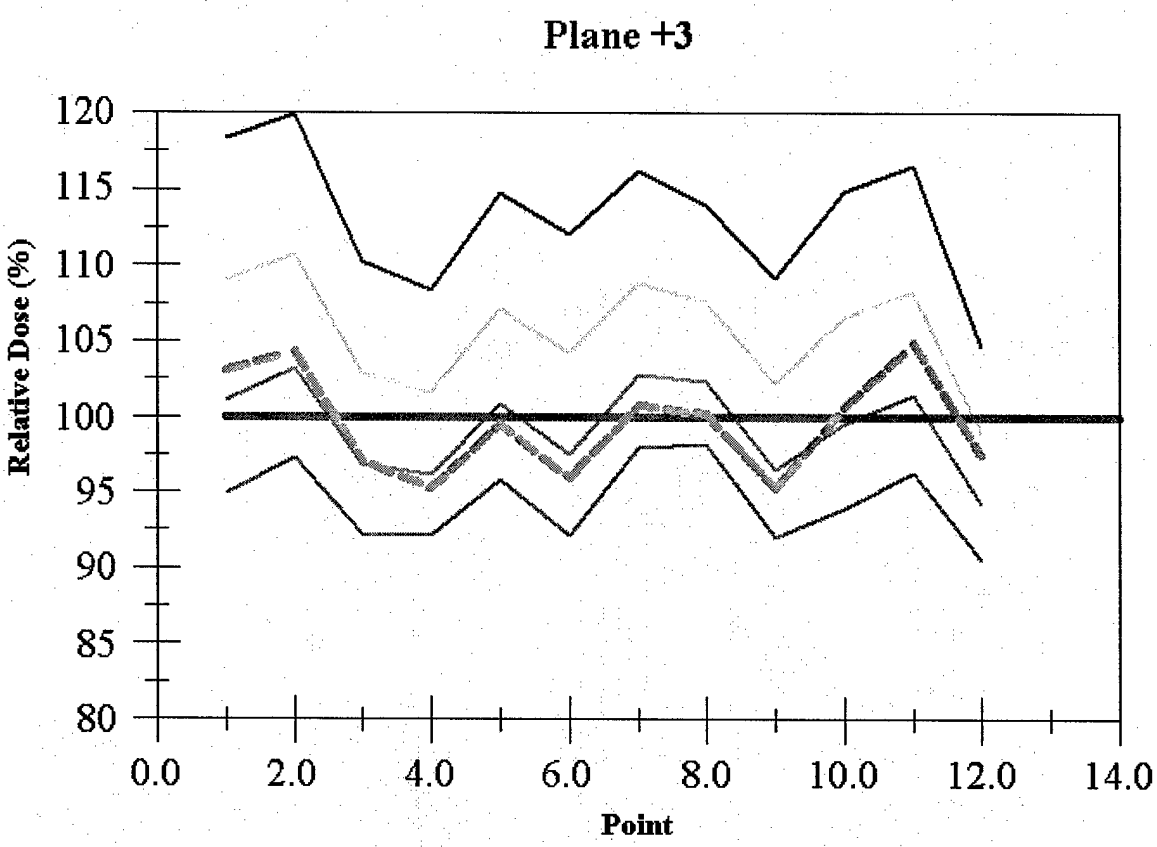

Figure 6: Dose profile in +3 cm plane for arcs defined using 3 cm, 4 cm, 5 cm, and 6 cm wide rectangular fields. The solid horizontal line corresponds to the "ideal" dose distribution in this plane (100% at all reference points). The dashed line corresponds to the "gross optimization" dose distribution in this plane. Notice that in this plane, only 3 cm above the central axis plane, the MLC leaf opening is basically reduced to 4 cm wide.

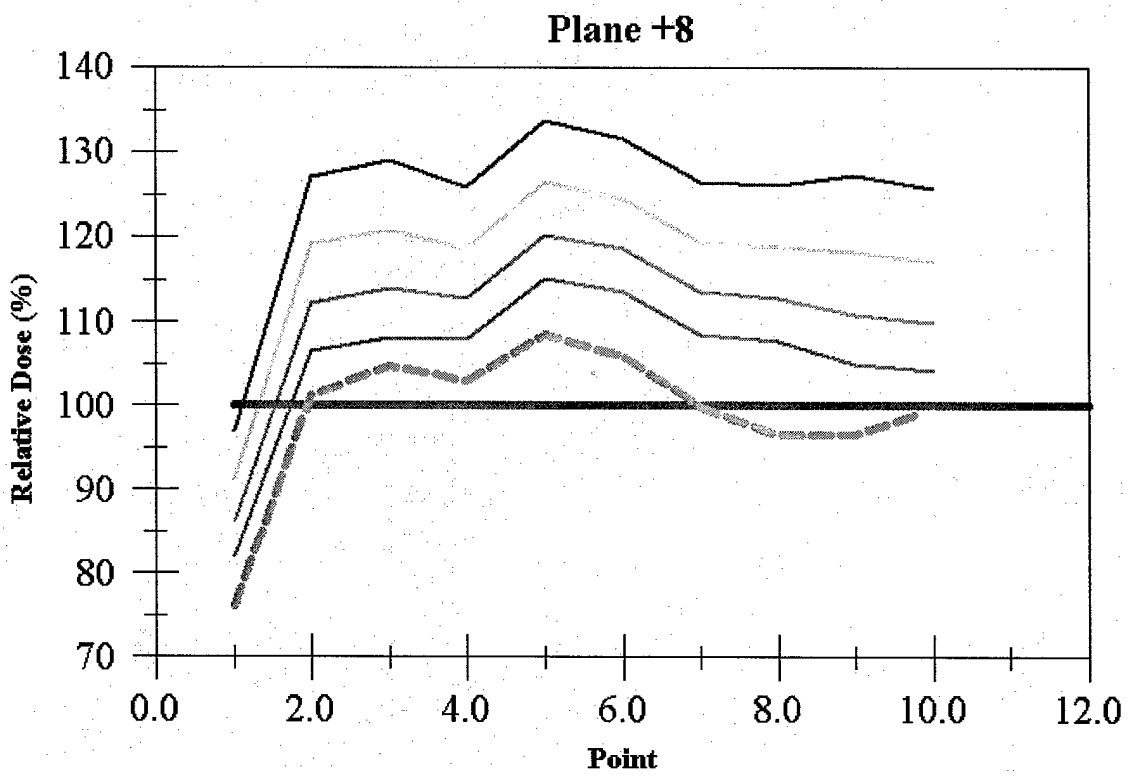

Figure 7: Dose profile in +8 cm plane for arcs defined using 3 cm, 4 cm, 5 cm, and 6 cm wide rectangular fields. The solid horizontal line corresponds to the "ideal" dose distribution in this plane (100% at all reference points). The dashed line corresponds to the "gross optimization" dose distribution in this plane. Notice that in this plane, the projected aperture width defined by the MLC leaves must be reduced to less than 3 cm. This reflects the smaller patient thickness in this superior plane, as well as electron scatter from the neighboring planes.

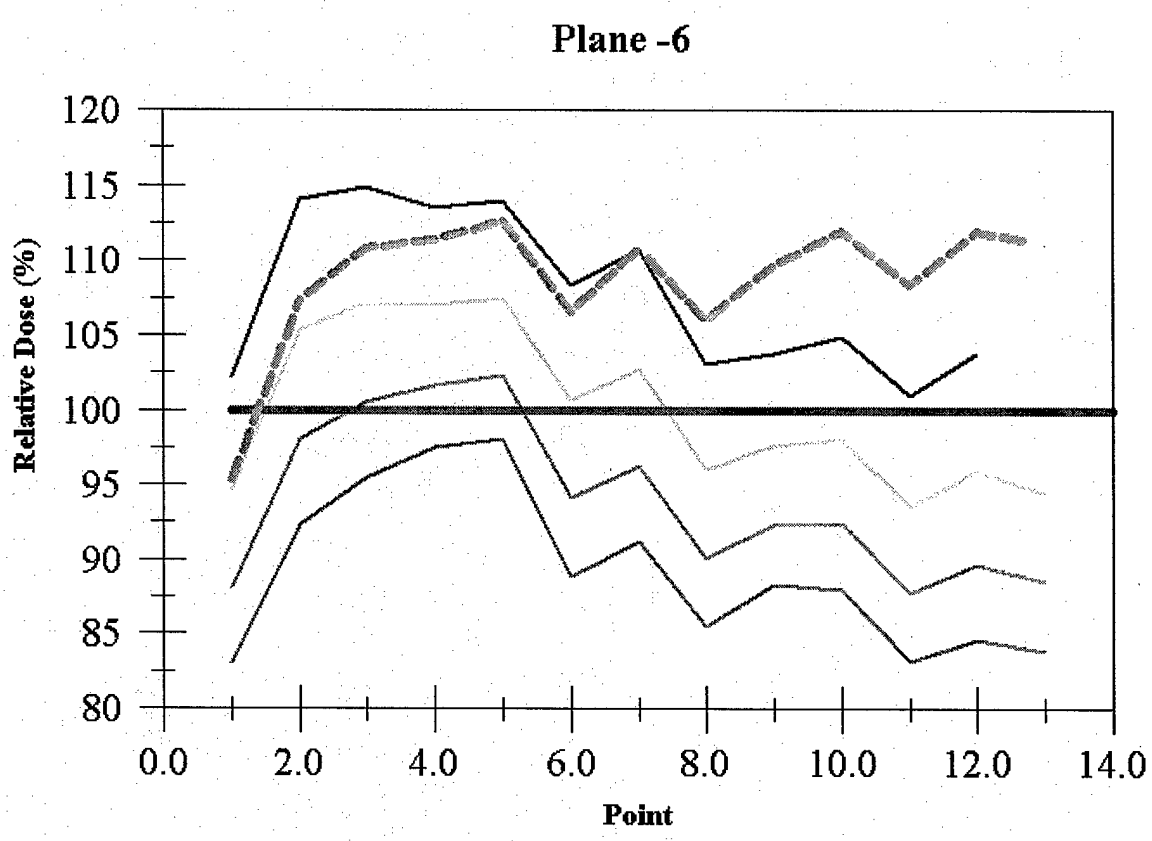

Figure 8: Dose Profile display for plane -6 cm below the central plane. Here the "Gross Optimization" technique failed, since it could not determine the exact plane from which to extract the arc field widths. This must be remedied with further insights.

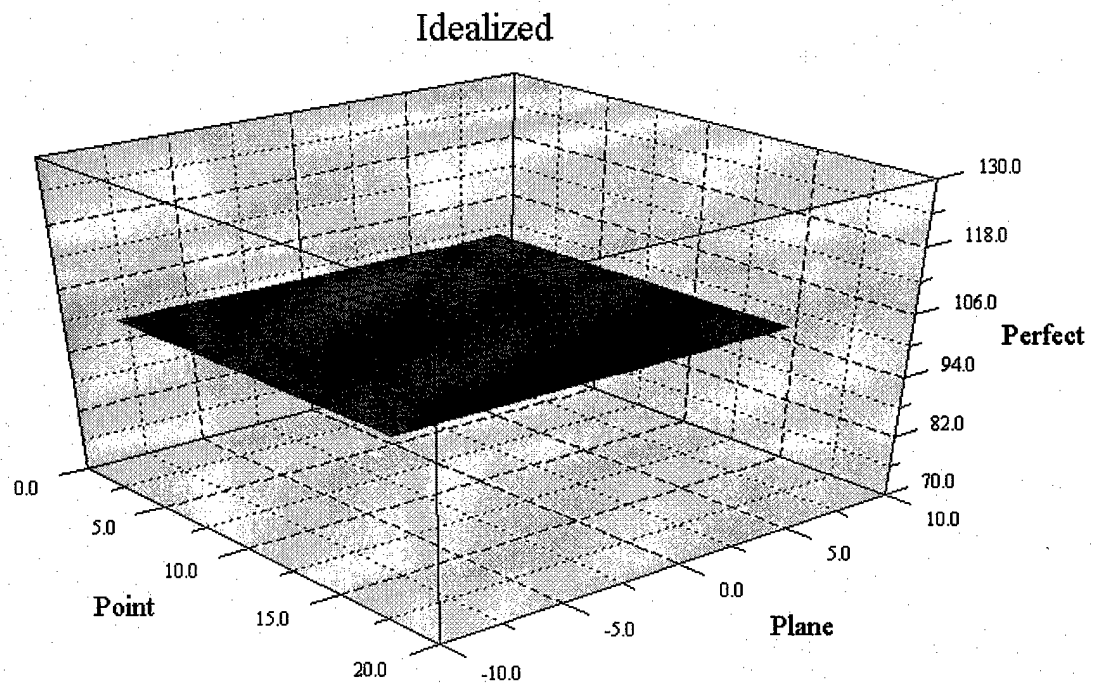

Figure 9: Dose surface map showing "Idealized" dose distribution (all dose points receiving 100% dose). The "Point" axis represents the reference points distributed across the arc in each plane; the "Plane" axis represents the planes from -8.5 cm to +8.5 cm in which dose calculations were done; and the "Perfect" axis represents the dose at each reference point. The "Idealized" dose distribution is presented as a horizontal plane, indicating that all points are receiving the 100% dose.

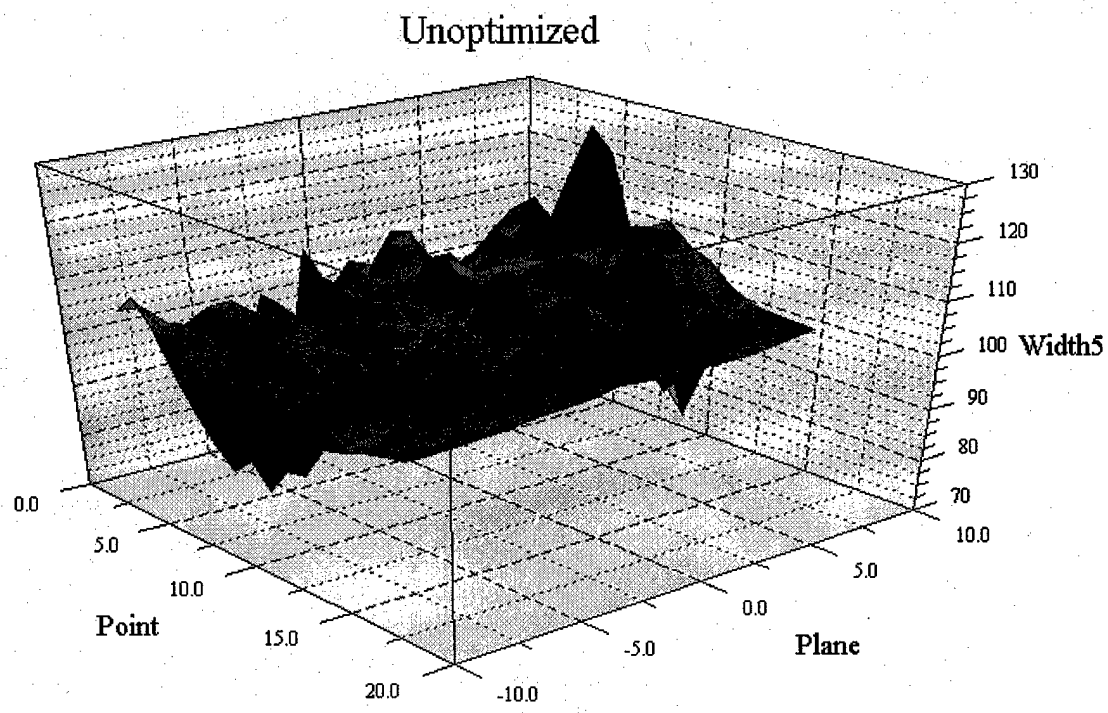

Figure 10: Dose surface map showing dose distribution resulting from use of 5 cm wide electron arc field across the entire arc. Notice the general trend of dose greater than desired in planes superior to the central axis, and less than desired in planes inferior to the central axis. There are exceptions to this, however, as is noted by the excursions to doses greater than 120% and less than 80% of desired dose.

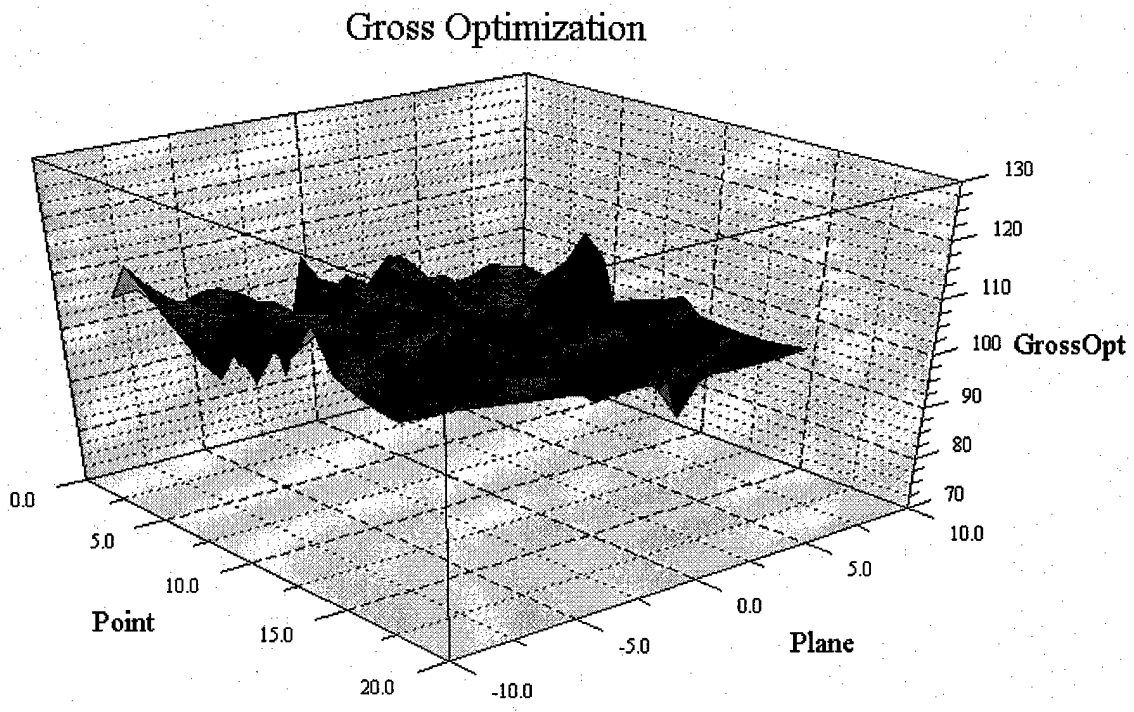

Figure 11: Dose surface map showing dose distribution resulting from use of field shapes predicted by "Gross Optimization" technique. Notice that the general trend of dose greater than desired in planes superior to the central axis, and less than desired in planes inferior to the central axis, has been reversed. The "Gross Optimization" technique is predicting fields that are slightly too narrow in the superior planes and slightly too wide in the inferior planes. This results because the "Gross Optimization" technique does not take into account the change in electron scatter contribution from the planes immediately superior and inferior to the plane of interest, but rather calculates contributions from all other planes as if they had the same field widths seen in the plane of interest.